

RSC Advances

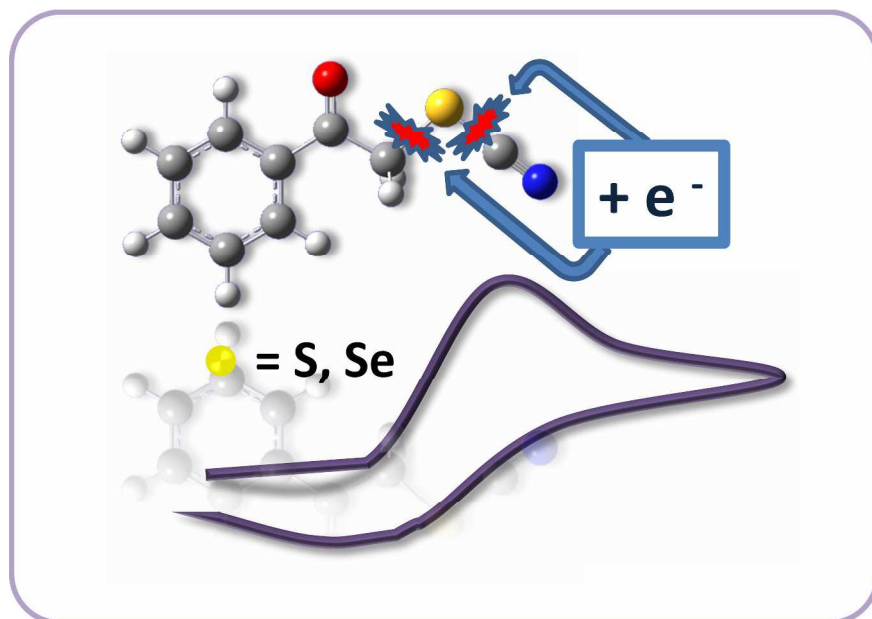


This is an *Accepted Manuscript*, which has been through the Royal Society of Chemistry peer review process and has been accepted for publication.

Accepted Manuscripts are published online shortly after acceptance, before technical editing, formatting and proof reading. Using this free service, authors can make their results available to the community, in citable form, before we publish the edited article. This *Accepted Manuscript* will be replaced by the edited, formatted and paginated article as soon as this is available.

You can find more information about *Accepted Manuscripts* in the [Information for Authors](#).

Please note that technical editing may introduce minor changes to the text and/or graphics, which may alter content. The journal's standard [Terms & Conditions](#) and the [Ethical guidelines](#) still apply. In no event shall the Royal Society of Chemistry be held responsible for any errors or omissions in this *Accepted Manuscript* or any consequences arising from the use of any information it contains.



Cite this: DOI: 10.1039/c0xx00000x

www.rsc.org/xxxxxx

ARTICLE TYPE

Breaking bonds with electrons: stepwise and concerted reductive cleavage of C-S, C-Se and Se-CN bonds in phenacylthiocyanates and phenacylselenocyanates

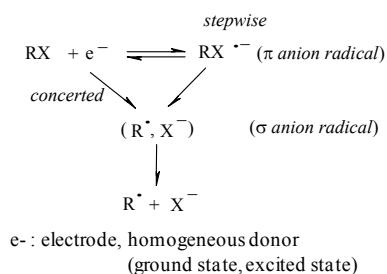
Lydia M. Bouchet,^a Alicia B. Peñéñory,^a Marc Robert^{*b} and Juan E. Argüello^{*a}

Received (in XXX, XXX) XthXXXXXXXXXX 20XX, Accepted Xth XXXXXXXXXXXX 20XX
DOI: 10.1039/b000000x

The mechanistic aspects of the electrochemical reduction of phenacylthio- and selenocyanates have been studied. With phenacylthiocyanates (**1**), a change in the reductive cleavage mechanism is observed as a function of the substituent on the phenyl ring. While a stepwise mechanism involving the intermediacy of a radical anion is followed for substrates bearing a strong electron withdrawing group such as cyano and nitro substituent (**1d**, **1e**), a concerted mechanism is favoured for compounds bearing an electron-donating or no substituent on the phenyl ring (**1a-c**). A regioselective bond cleavage leads to fragmentation of the CH₂-S bond with all compounds **1a-e**, further yielding the corresponding 1,4-diketone (**3**) as products. Contrastingly, with phenacylselenocyanates (**2**), two different reductive cleavages occur involving breaking of both the CH₂-Se and Se-CN bonds. Several products are obtained, all coming from nucleophilic attack at the α (phenacyl) carbon or the selenium atom.

Introduction

The coupling between charge transfer and bond cleavage between two heavy atoms occurs in a large number of chemical, biochemical and catalytic processes, such as cleavage of C-halogen bonds in organic halides as well as other bonds,¹⁻⁴ electron transfer activation of small molecules involved in contemporary energy challenges (such as e.g. H₂O, O₂, N₂ and CO₂), as well as enzymatic reactions like dechlorination processes of RX (X = Cl) toxic derivatives within reductive dehalogenases.⁵ In these reactions, the cleavage accompanying charge transfer may be triggered in various ways, electrochemically, by homogenous electron donors or acceptors, photochemically or by means of pulse radiolysis.¹⁻³ Charge transfer and bond cleavage reaction may occur concertedly according to a single elementary step (concerted dissociative electron transfer), or in two successive steps, the electron transfer then generating a frangible species that reacts in a distinct, chemical step, as shown in Scheme 1.¹⁻³



Scheme 1 Dissociative electron transfer mechanisms for the reduction of a substrate RX.

Potential energy curves describing both reactant and products are modelled by Morse curves, with the assumption that the repulsive interaction of the two fragments formed upon charge transfer is identical to the repulsive part of the reactant Morse curve.⁶ Solvent reorganization is calculated from the Marcus-Hush model. These two ingredients of the model lead to a quadratic activation (activation free energy: ΔG^\ddagger) - driving force (minus standard free energy: $-\Delta G^0$) relationship as given in equation (1):¹⁻³

$$\Delta G^\ddagger = \frac{D_{\text{RX}} + \lambda_0}{4} \left(1 + \frac{\Delta G^0}{D_{\text{RX}} + \lambda_0} \right)^2 \quad (1)$$

where D_{RX} is the homolytic bond dissociation energy and λ_0 the solvent reorganization energy. The standard free energy of the reaction leading to complete dissociation (E : electrode potential, $E_{\text{RX/R}^\bullet + \text{X}^-}^0$: standard potential of the RX / R[•] + X⁻ couple) is given by

$$\Delta G^0 = F(E - E_{\text{RX/R}^\bullet + \text{X}^-}^0) = F(E + D_{\text{RX}} - T\Delta S^0 - E_{\text{X}^\bullet/\text{X}^-}^0) \quad (2)$$

where $E_{\text{X}^\bullet/\text{X}^-}^0$ is the standard potential of the X[•] / X⁻ redox couple and ΔS^0 is the bond dissociation entropy and, when required, additional sources of intramolecular reorganization may be included as an additive term to the intrinsic barrier:

$$\Delta G_0^\ddagger = \frac{D_{\text{RX}} + \lambda_0}{4} \quad (3)$$

The homolytic bond dissociation energy D_{RX} represents the kinetic penalty for the concerted reaction as compared to the

sequential pathway. The electron transfer rates may then be expressed as in the Marcus-Hush theory (equation 4):⁷⁻¹¹

$$k(E) = Z \exp \left[-\frac{D_{RX} + \lambda_0}{4RT} \left(1 + \frac{F(E - E_{RX/R^+X^-}^0)}{D_{RX} + \lambda_0} \right)^2 \right] \quad (4)$$

where Z is the pre-exponential factor.

This set of equations has been applied with success to both homogeneous and heterogeneous concerted dissociative electron transfers (in the former case, the electrode potential in the driving force expression should be replaced by the standard potential of the molecular electron donor), including for C-halogen bonds (alkyl and benzyl halides),^{6, 12-14} O-O bonds (alkyl peroxides),^{15, 16} but also N-halogen bonds (N-halogenosulfams),¹⁷ N-S bonds (sulfonylphthalimides),¹⁸ S-C bonds (sulfoniumcations)¹⁹ or S-Cl bonds in arenesulfonyl chlorides.^{20, 21} It also allowed identifying the competition that exists between the concerted and stepwise pathways, and depends upon intramolecular (structural, electronic) and environmental (solvent, energy of the incoming electron) factors.

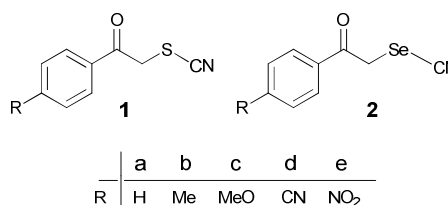
Focusing on C-S bonds, the electrochemical reduction of various substituted benzyl thiocyanates showed a change in the cleavage mechanism as a function of the substituent on the benzyl ring.^{1, 22, 23} For the *p*-nitrobenzylthiocyanate, a stepwise dissociative electron transfer mechanism with an anion radical as intermediate takes place, the electron being transiently located on the π^* orbital (largely localized on the nitro groups), before cleavage occurs at the C-S bond. The reduction of the *p*-cyanobenzylthiocyanate follows a concerted charge transfer-bond breaking mechanism, with the electron going directly in the σ^* orbital of the C-S bond. With benzyl thiocyanate, the reduction is also concerted with bond cleavage, but cleavage occurs both at the C-S bond (α -cleavage) and at the S-CN bond (β -cleavage).^{22, 24}

In the case of phenacylthiocyanates, it has been proposed that cathodic reduction at a controlled potential releases ^-SCN as a leaving group and that after a second electron transfer an enolate ion is formed.²⁵ This electrogenerated enolate anion acts as a nucleophile to give a 1,4-diketone as the main product. No mechanistic details have been given about the intimate mechanisms for electron transfer and subsequent reactions, notably the degree of association between charge transfer and bond cleavage. On the other hand, the behaviour of phenacylselenocyanates differs from the corresponding sulphur one, since the organic selenocyanates undergo a displacement of the CN group by attack of nucleophilic reagents. It was suggested that the electrogenerated enolate anion formed after cleavage of the C-Se bond and reduction with a second electron attacks the phenacylselenocyanate to render the (2-phenacylseleno)acetophenone as the main product.²⁶ Again, no detailed mechanisms were provided.

In this report, we describe the electrochemical reduction of different phenacylthiocyanates (**1**) and phenacylselenocyanates (**2**). The SCN and SeCN groups of **1** and **2** may be considered as pseudohalogen groups. These functional groups can also be used as a masked mercapto/seleno group, as well as precursors toward the synthesis of sulphur/selenium-containing organic compounds. These later compounds possess a broad range of bioactivities

with applications as anticancer agents, and their redox behavior is also interesting since some of them exhibit glutathione peroxidase (GPx) activity.²⁷⁻²⁹

Using both, cyclic voltammetry (CV), theoretical calculations and the model for concerted dissociative electron transfer, we have determined the concerted or stepwise nature of the bond breaking processes and provided a complete analysis of the reduction processes. Various regioselectivity and various mechanisms were encountered. The selected compounds for this study bearing electron donor and withdrawing groups are shown below (Scheme 2).



Scheme 2 Phenacylthiocyanates and phenacylselenocyanates investigated.

Results and Discussion

Phenacylthiocyanates (**1**) and phenacylselenocyanates (**2**) were prepared according to standard procedures. Full characterization of new compounds **1d** and **2d** can be found in the Experimental Section and in the Supporting Information (NMR spectra). The mechanistic analysis was based on the use of the concerted dissociative electron transfer model, in conjunction with insights issued from DFT quantum chemical calculation.

Electrochemical reduction of phenacylthiocyanates (1a-e)

The electrochemical reduction of the phenacylthiocyanates (**1a-e**) was studied by cyclic voltammetry (CV) in *N,N'*-dimethylformamide (DMF), in the presence of tetrabutylammoniumtetrafluoroborate (TBAF, 0.1 M) at a glassy carbon electrode. In all cases, the first cathodic wave does correspond to the cleavage of the CH₂-S bond (see below), showing a remarkable regioselectivity for cleavage in the whole family. The peak characteristics (peak potential (E_p), peak width ($E_p - E_{p/2}$), slope of E_p vs. $\log(\nu)$ where ν is the scan rate, number of electrons per molecule, and transfer coefficient (α_p)) were obtained for all of these compounds and are given in Table 1.^{30, 31} As an example, the CV of phenacylthiocyanate **1a** in DMF displays an irreversible reduction peak at -1.29 V vs SCE at low scan rate (Figure 1a). The peak width has a value of 103 mV and the peak potential varies linearly with $\log(\nu)$ with a slope of 63 mV (Figure 1b). The transfer coefficient (α_p) values, obtained from peak width (0.46) and from the slope of $\delta E/\delta \log(\nu)$ (0.47), are indicative of a slow electron transfer.^{1, 2} This first reduction peak corresponds to the consumption of one electron per molecule (by comparison to the mono-electronic wave of ferrocene and taking into account the slow charge transfer). Scanning in the oxidative direction after the first peak allows observing an oxidation wave ($E_p = 0.79$ V vs. SCE) similar to the oxidation of $^+NH_4$, ^-SCN ($E_p = 0.78$ V vs. SCE at low scan rate), showing that the thiocyanate anion is formed and thus that the CH₂-S bond is broken during the reduction process. A second reduction peak (reversible) can be seen at lower potentials (-2.03

V vs. SCE at low scan rate, Figure 1a). As shown in Figure 2, it may correspond to the reduction of acetophenone or alternatively to the reduction of the dimer 1,4-diphenyl-1,4-butanedione (**3a**). It has indeed been reported²⁵ that the most likely reduction product of **1a** in DMF is the 1,4-diphenyl-1,4-butanedione (**3a**), since the carbon centred radical formed after the CH₂-S fragmentation is immediately reduced at the electrode surface, yielding the corresponding enolate anion which acts as nucleophile in a subsequent addition process (Scheme 3). This second reduction peak provides a further proof that the CH₂-S bond fragments upon reduction.

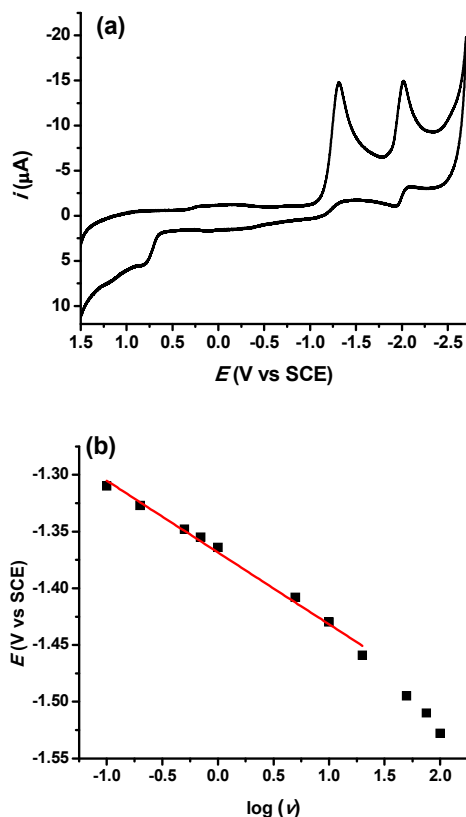


Fig. 1 (a) CV of **1a** (1 mM) in DMF + TBAF (0.1 M) at a glassy carbon electrode, $\nu = 0.1 \text{ Vs}^{-1}$. (b) Variation of the peak potential (1st reduction wave) with scan rate.

Compounds **1b** and **1c** show similar reduction features with a first, broad, mono electronic reduction peak characterized by slow electron transfer (Figure S1 and Table 1) and negative reduction potentials (-1.36 to -1.40 V vs SCE at low scan rates). The transfer coefficient values determined from the peak width

Table 1 Electrochemical characteristics of CVs for substituted phenacylthiocyanates (**1**)

ArCOCH ₂ SCN ^a	$E_{p,1}^b$ (V vs SCE)	n^c	$\delta E_p / \delta \log(\nu)$ slope ^d	α_p^e	$E_{p,2} - E_p$ (mV)	α_p^f	$E_{p,2}^g$ (V vs SCE)	E_p ArCOCH ₃
1a	-1.29	1.2	-63	0.47	103	0.46	-2.03	-2.03
1b	-1.36	0.9	-79	0.37	102	0.46	-2.10	-2.13
1c	-1.39	0.9	-76	0.39	127	0.37	-2.16	-2.19
1d	-0.97	1.2	-59	0.5	80	0.59	-1.47	-1.45

^aIn DMF, TBAF (0.1M), [**1a-e**] = 1 mM. ^bFirst reduction peak potential at 0.1 V.s⁻¹. ^cNumber of electrons exchanged per molecule. ^dmV per unit log(ν).

^eFrom $E_{p,1}$ vs log(ν). ^fFrom peak width. ^gSecond reduction peak potential.

and from the slope of E_p vs log(ν) plot are 0.46 and 0.37 for **1b**, 0.37 and 0.39 for **1c**, respectively. As with **1a**, the reduction leads to CH₂-S bond fragmentation. The first cathodic peak is followed by a second peak (Table 1), corresponding to the reduction of the 1,4-diketones (1,4-bis(4-tolylbutane-1,4-dione for **1b** and 1,4-bis(4-methoxyphenyl)butane-1,4-dione for **1c**) obtained after nucleophilic attack of the electrogenerated enolate onto reactant substrates **1b-c** (Scheme 3), similarly to the mechanism followed with **1a**.

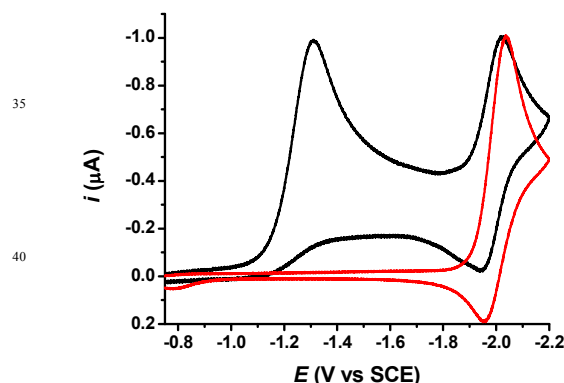


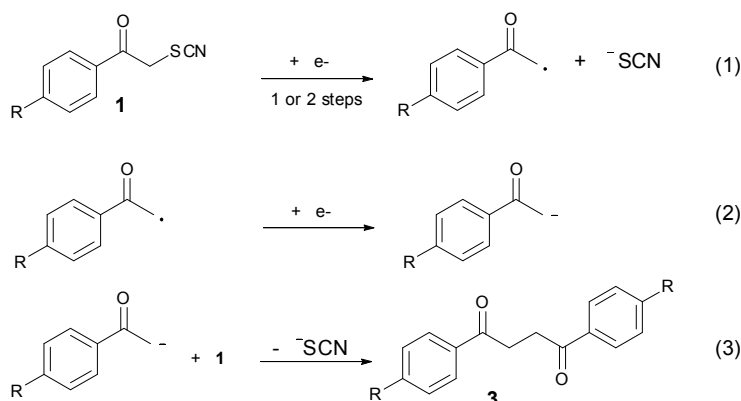
Fig. 2 Cyclic voltammetry of **1a** (1 mM, -) and acetophenone (1 mM, -) in DMF + TBAF (0.1 M) at a glassy carbon electrode, $\nu = 0.1 \text{ Vs}^{-1}$.

Compounds **1d** and **1e** display a similar reduction pattern with a first monoelectronic, irreversible reduction peak, but at potentials much more positive than those measured with **1a-c** (-0.97 V for **1d** and -0.64 V vs SCE for **1e**, see Table 1 and Figure S1). This first reduction wave is also characterized by much smaller peak widths (between 60 mV and 80 mV at low scan rates) and smaller peak potential variations with the scan rate (Table 1), indicative of larger transfer coefficient and faster electron transfer. The CH₂-S bond is broken along the reduction wave, as with **1a-c**. However CV's characteristics clearly point toward a different mechanism for cleavage. A second, more negative wave is observed (see Table 1) corresponding to the reduction of 1,4-bis(4-cyanophenyl)butane-1,4-dione (**3d**) and 1,4-bis(4-nitrophenyl)butane-1,4-dione (**3e**), respectively, again similarly to compounds **1a-c** (Scheme 3). Further cathodic waves are observed at more negative potentials, due to multielectronic reduction processes of the aromatics (see supporting information, Figure S1).

Cite this: DOI: 10.1039/c0xx00000x

www.rsc.org/xxxxxx

ARTICLE TYPE



Scheme 3 Electrochemical one electron reduction mechanism for phenacylthiocyanates 1a-e.

Note that in the presence of an excess of phenol, all compounds **1a-e** show a two electrons stoichiometry at the first reduction peak, in agreement with the proposed reaction mechanism (Scheme 3), where the enolate is intercepted by the acidic phenol before acting as a nucleophilic agent towards a neutral substrate molecule, thus leading to the use of two electrons per reactant molecule (reactions (1) + (2) in Scheme 3). Note also that these results are in agreement with those previously reported.²⁵

Mechanisms for the C-S bond fragmentation

The C-S bond breaking (reaction (1), Scheme 3) may occur in one concerted step or sequentially in two steps through the formation of a transient radical anion, which further undergoes cleavage in a second elementary step. Combining DFT calculations, analysis of CV characteristics and application of the model for concerted dissociative electron transfer allows getting insights in the mechanism as a function of the substituent on the phenyl ring. In the cases of **1a** (Figure 3), **1b** and **1c**, we were unable to find any minima on the potential energy surface that would correspond to the formation of a radical anion intermediate. Instead, fragmentation occurs at the CH₂-S bond, in agreement with experiments, and a loose adduct between the two fragments, the phenacyl radical and the thiocyanate anion, was identified, as shown for **1a** in Figure 3 (left). In contrast, with compounds **1d** (Figure 3, right) and **1e**, a minimum was found prior bond breaking, that corresponds to the formation of a radical anion intermediate, with the electronic density mainly localized on the electron withdrawing group borne by the phenyl group (CN for **1d**, NO₂ for **1e**). For compounds **1d** and **1e**, electrochemical data (Table 1) are in agreement with an *E* + *C* mechanism, where a first electron transfer (*E*) is followed by a fast chemical reaction (*C*), the breaking of the C-S bond. DFT calculations further confirm the occurrence of a stepwise mechanism. In other words, reaction (1) (Scheme 3) takes place in two elementary steps. The initial electron is mainly located on the low lying π* orbital of the phenyl ring, thanks to the electronic withdrawing substituents (CN, NO₂).

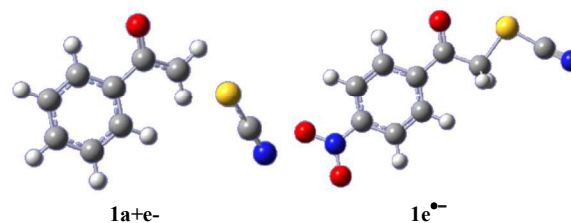


Fig. 3 Left: [phenacyl radical / thiocyanate anion] adduct obtained upon reduction of **1a**. Right: **1e**^{•-} radical anion. Gray : carbon; white : hydrogen; red : oxygen; blue : nitrogen; gold : sulphur.

This thermodynamic effect reflects in the peak potentials that are largely positive to the peaks obtained with compounds **1a-c** (the positive shift is roughly 400 mV with **1d** and 700 mV with **1e** as compared to average peak potential values obtained for **1a-c**). For compounds **1a-c**, DFT calculations suggest a different mechanism, involving a concerted reduction-bond breaking process of the neutral substrate (reaction (1) in Scheme 3 occurs through one single step). The two fragments issued from cleavage, the phenacyl radical on one hand and the thiocyanate anion on the other hand, are weakly interacting in the gas phase (as illustrated for **1a** in Figure 3). This weak charge-dipole interaction is likely to be washed out in polar DMF. The CV characteristics are compatible with such a mechanism (Table 1), notably the low values for the electron transfer α, suggesting high values for the reorganization energy. However, more evidence needs to be gathered in order to conclude about the exact mechanism. By using the model for concerted dissociative electron transfer, we may evaluate the transfer coefficient values and compare them to the experimental values. Transfer coefficient is defined through equation (5):

$$\alpha = \frac{\partial \Delta G^\ddagger}{\partial \Delta G^0} = \frac{1}{2} \left(1 + \frac{\Delta G^0}{4\Delta G_0^\ddagger} \right) \quad (5)$$

where ΔG[‡] is the activation free energy, ΔG⁰ is the standard free

energy and ΔG^\ddagger_0 is the standard free activation energy obtained at zero driving force. The standard free energy of the reaction leading to complete dissociation is given by equation (2). In this equation as well as in equation (1), E is the electrode potential, D_{RX} is the homolytic bond dissociation energy (C-S bond), ΔS^0 is the bond dissociation entropy and $E^0_{X^+/X^-}$ is the standard potential of the X^+ / X^- redox couple ($X = SCN$). This last parameter is equal to 0.75 V vs. SCE.²⁴ λ_0 , the solvent reorganization energy, could be estimated through the equivalent radii a of the substrate ($\lambda_0 \approx 3/a$).^{1, 2} The homolytic bond dissociation energy D_{RX} (C-S bond) and bond dissociation entropy were evaluated by DFT calculations. It also leads to the obtention of the standard free activation energy (intrinsic barrier) through equation (3). All data for compounds **1a-c** are given in Table 2.

Table 2 Thermodynamic parameters for the reduction of phenacylthiocyanates **1a-c**.

$RC_6H_4COCH_2SCN$	E_p^a	D_{RX}^b	ΔS^0 ; $T\Delta S^0^d$	a^c	λ_0^d
1a R = H	-1.29	46	40.1 ; 0.52	4.5	0.66
1b R = CH ₃	-1.36	45.9	41.0 ; 0.50	4.7	0.64
1c R = OCH ₃	-1.39	45.7	40.4 ; 0.52	4.7	0.64

^aV vs SCE at 0.1 V.s⁻¹. ^bkcal mol⁻¹. ^ccal mol⁻¹. ^deV. ^eÅ.

With these parameters in hands, we were then able to estimate ΔG^0 , ΔG^\ddagger at the CV peaks, and then to calculate α . The results obtained at low scan rates are presented in Table 3. A good quantitative match between the experimental (α_{exp}) and calculated (α_{calc}) values is obtained, thus validating a concerted reductive cleavage mechanism of the C-S bond upon first electron reduction. The electron directly goes into the σ^* orbital of the carbon-sulphur bond, since no low energy hosting orbital is available for generating a radical anion intermediate, in contrast with what is observed for **1d** and **1e**. The very negative reduction potentials (as compared to those measured with **1d** and **1e**) were already clues that the mechanism was likely to be concerted. The single use of DFT calculations can not lead to the reduction mechanisms, in particular because micro-solvation of the charged species (leaving anion, radical and radical anions) can not be reproduced accurately, however they provide a useful tool for confirming that the mechanisms drawn from cyclic voltammetry studies are coherent and plausible.

Table 3 Thermodynamic and kinetic parameters for the reduction of phenacylthiocyanates **1a-c**.

$RC_6H_4COCH_2SCN$	ΔG^0 ^a	ΔG^\ddagger_0 ^a	α_{calc}	α_{exp} ^b
1a R = H	-0.564	0.663	0.40	0.47
1b R = CH ₃	-0.601	0.657	0.38	0.37
1c R = OCH ₃	-0.682	0.655	0.37	0.39

^a in V, calculated from equation (2) and (3) at the peak potential (for $v = 0.1$ V s⁻¹). ^b from Table 1, values obtained from the variation of E_p with $\log(v)$.

Electrochemical reduction of phenacylselenocyanates (**2**)

The electrochemical reduction of the phenacylselenocyanates (**2a-e**) was studied by CV in DMF + TBAF 0.1 M at a glassy carbon electrode. Characteristics for reductive peaks were determined and the results are summarized in Table 4.

The CV of phenacylselenocyanate (**2a**) displays an irreversible reduction peak at a potential $E_p = -1.08$ V vs SCE (Figure 4), with a shoulder close to -0.89 V vs SCE (indicated as $E_{shoulder}$ in Table

4). The irreversible peak observed at -2 V vs SCE corresponds to the reduction of 1,4-bisphenylbutane-1,4-dione (**3a**) (or to the reduction of the substituted acetophenone), as observed in the case of thiocyanate analogue. Cleavage of the CH₂-Se bond is thus likely to occur at the first reduction peak. That selenocyanate anion is the leaving group was confirmed by the observation of an oxidation wave ($E_p = 0.59$ V vs SCE) similar to that of K⁺, ⁻SeCN ($E_p = 0.53$ V vs SCE). The phenacyl radical PhCOCH₂• obtained after cleavage is reduced at the electrode to the ketone enolate anion (PhCOCH₂⁻) with a second electron, and this enolate ion reacts with a neutral reactant to provide **3a** (Scheme 4). Another smaller reduction peak is observed at a potential close to -1.48 V vs. SCE (Table 4, Figure 4). It is ascribed to the reduction of the selenide **4a** (2-(phenacylseleno)acetophenone), which was identified by comparison with an authentic sample (see supporting information, Figure S5). This result is in agreement with previous studies,²⁶ where selenide **4a** may come from nucleophilic attack of the enolate at the selenium atom while releasing cyanide ion as leaving group, as shown on Scheme 4. Alternatively, **4a** may come from a nucleophilic addition of a selenate anion (PhCOCH₂Se⁻) onto **2a** (Scheme 4). Such a selenate anion could be formed upon cleavage of the Se-CN bond (Scheme 4). The observation of a shoulder just before the main, first reduction peak may be the signature of this reductive cleavage (that does not occur in the thiocyanate family of compounds). Breaking of the Se-CN bond may also lead to the dimer compound **5a** (2,2'-diselenediylbis(1-phenylethanone), Scheme 4) by a nucleophilic reaction of the selenate anion at the selenium atom of reactant **2a**. CV of an authentic sample of diselenide **5a** indicates that once formed, it is reduced to **4a** (see supporting information, Figure S5).

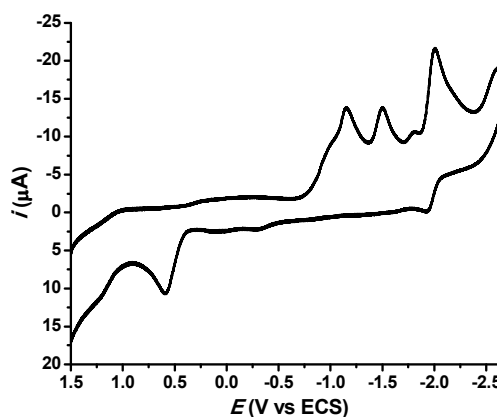


Fig. 4 Cyclic voltammetry of **2a** (1 mM) in DMF + TBAF 0.1M, $v = 0.1$ V s⁻¹.

In total, reduction of **2a** leads to the cleavage of the CH₂-Se bond and to the cleavage of the Se-CN bond, as illustrated on Scheme 4. This non-regioselective reduction process as compared to sulphide analogue **1a** may be ascribed to the fact that the Se-CN cleavage, despite the large Se-CN homolytic bond dissociation energy, may be significantly accelerated by in-cage interactions between the fragments PhCOCH₂Se• and CN⁻ (charge-dipole interaction). Although studies of these interactions stands beyond the scope of this paper, preliminary quantum calculations indicate that a significant attractive interaction (typically in the order of

0.1 eV) does exist between the selenium centred radical and the cyanide anion, while for the CH₂-Se bond cleavage, there is no interaction between the phenacyl radical and the selenocyanate anion. Note that a sticky interaction in the order of only 1% of $D_{\text{C-Se}}$ will result in a decrease of about 15% of the intrinsic barrier for concerted reductive cleavage.² Thus even if the CH₂-Se bond breaking is favoured because of a smaller homolytic bond dissociation energy ($D_{\text{CH}_2\text{-Se}} = 44 \text{ kcal mol}^{-1} \ll D_{\text{Se-CN}} = 90.7 \text{ kcal mol}^{-1}$, estimated by DFT calculations) both cleavages are observed.

Compounds **2b** and **2c** show similar peak characteristics (see supporting information, Figure S4) to compound **2a**. In particular they all present a first reduction peaks with a shoulder at lower potentials (Table 4). This first peak is followed by a second irreversible peak (-1.54 V vs. SCE for **2b** and -1.63 V vs. SCE for **2c**), in agreement with the reduction of the corresponding selenides with retention of the Se atom (compounds **4b** and **4c**, Scheme 4). Then a third irreversible reduction peak corresponding to the reduction of 1,4-bis(4-tolyl)butane-1,4-dione (**3b**) (starting from **2b**) and 1,4-bis(4-methoxyphenyl)butane-1,4-dione (**3c**) (starting from **2c**) could be seen on the CVs. All of these products resulted from nucleophilic attacks as illustrated in Scheme 4. Compound **2d** shows comparable characteristic peaks to **2a-c** compounds (see supporting information, Figure S4), except that the two reduction processes on the first cathodic wave (C-Se and Se-CN cleavages) almost merge, thus giving a very large peak width (125 mV). As a consequence, the reduction of **2d** leads to three products following nucleophilic reactions (Scheme 4).

In this case of *p*-nitrophenacylselenocyanate (**2e**), CVs display

only a first reduction peak corresponding to consumption of one electron per molecule at a potential of -0.57 V vs. SCE (Figure 5, Table 4), much more positive than with compounds **2a-c** (typically 300 to 500 mV more positive). At more cathodic potentials, several reduction waves are observed which correspond to the reduction of 1,4-bis(4-nitrophenyl)butane-1,4-dione (**3e**) and to further reduction of the nitrophenyl ring. Fragmentation of the C-Se bond occurs at the first cathodic peak with no cleavage of the Se-CN bond, because the reduction is driven to less negative potential due to the nitro substituent on the phenyl ring, making the Se-CN fragmentation non competitive.

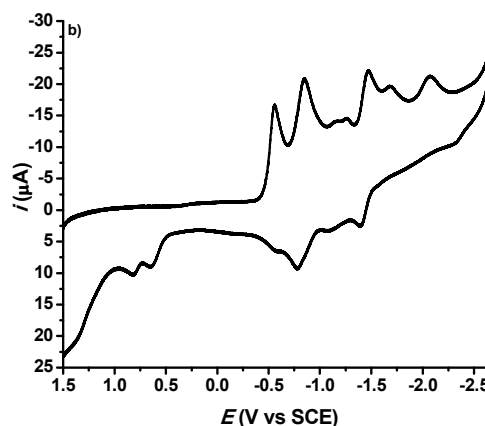
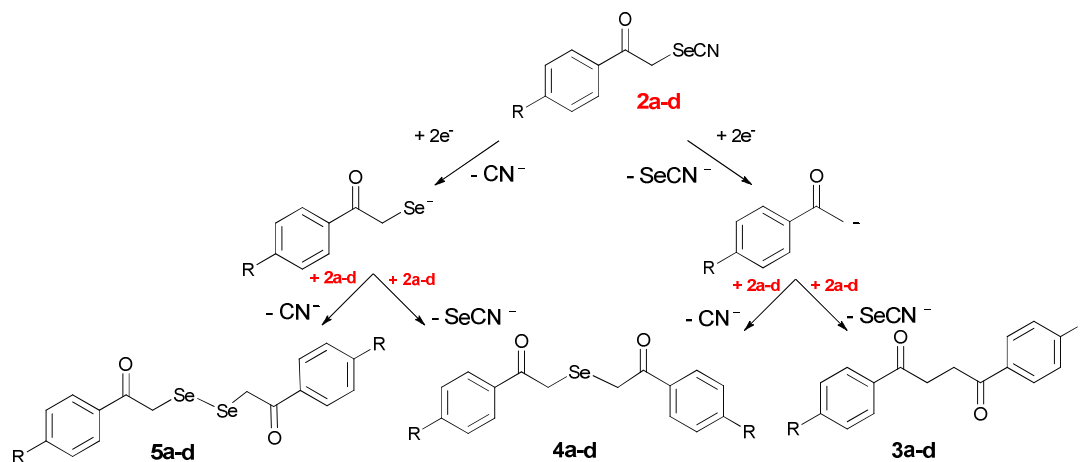


Fig. 5 Cyclic voltammetry of **2e** (1 mM) in DMF + TBAF 0.1 M, $\nu = 0.1 \text{ V s}^{-1}$.

Table 4 Electrochemical characteristics of CVs for substituted phenacylselenocyanates (**2**).

ArCOCH ₂ SeCN ^a	E_{shoulder} (V vs ECS)	E_{p1}^{b} (V vs SCE)	$\delta E_{\text{p}}/\delta \log(\nu)^{\text{c}}$	$E_{\text{p2}} - E_{\text{p}}^{\text{d}}$ (mV)	E_{p2}^{d} (V vs ECS)	E_{p3}^{e} (V vs SCE)
2a	-0.89	-1.08	-85	---	-1.48	-2.00
2b	-0.98	-1.09	-155	---	-1.54	-2.10
2c	-1.19	-1.29	-65	---	-1.63	-2.19
2d	---	-0.90	-64	125	-1.27	-1.48
2e	---	-0.57	-54	58	-0.84	-1.47

^ain DMF + TBAF (0.1M), [**2a-e**] = 1 mM. ^bFirst reduction peak potential. ^cmV per unit log (ν). ^dSecond reduction peak potential. ^eThird reduction peak potential.



Scheme 4 Mechanism for the electrochemical reduction of phenacylselenocyanates (**2a-d**)

Cite this: DOI: 10.1039/c0xx00000x

www.rsc.org/xxxxxx

ARTICLE TYPE

Conclusions

In conclusion, important mechanistic aspects of the electrochemical reduction of phenacylthio- and selenocyanates have been deciphered. With phenacylthiocyanates (**1**), a striking change in the reductive cleavage mechanism is observed as a function of the substituent on the phenyl ring. In the case of a cyano or a nitro substituent (**1d** and **1e**) a stepwise mechanism involving the intermediacy of the radical anion takes place, while a concerted mechanism is operative with compounds bearing an electron-donating (or no) substituent on the phenyl ring (**1a-c**). CV characteristics as well as analysis of the voltammograms in terms of transfer coefficient (α) and theoretical calculations both converge towards these conclusions. Remarkably, a regioselective bond cleavage is observed and reductive fragmentation of the CH₂-S bond is followed for all compounds **1a-e**, leading to the corresponding 1,4-diketone (**3**) as products. The later are formed by an electrochemical-chemical mechanism where the electrogenerated ketone enolate anions act as nucleophiles in substitution reactions toward **1a-e**, with thiocyanate anion as a leaving group. By contrast, forphenacylselenocyanates **2**, and except in the case of **2e** which reacts as the sulphur analogue, two different reductive cleavages occur involving breaking of both the C-Se and Se-CN bonds at closely positioned potentials, resulting in the obtention of several products, all coming from nucleophilic attack at the α (phenacyl) carbon or the selenium atom.

Experimental Section

General Methods

¹H, ¹³C and ⁷⁷Se NMR spectra were recorded at 400.16, 100.62 and 76.32 MHz respectively on a Bruker 400 spectrometer, and chemical shifts were reported in δ (ppm) relative to TMS with CDCl₃ as solvent. HRMS were recorded on a MicroTOF Q II equipment, operated with an ESI source and positive mode, using nitrogen as nebulising and drying gas and sodium formate 10 mM as internal calibrant.

Chemicals

Dimethylformamide (DMF, Aldrich, > 99.8%, extra dry over molecular sieves) was used without further purification. Commercially available reagents were used without further purification. Compounds **1a-e**³² and **2a-e**²⁶ were prepared following literature methods.

p-Cyanophenacylthiocyanate (**1d**)

White solid. ¹H NMR (400.16 MHz, CDCl₃, 25°C, TMS): δ = 8.05 (d, J = 8.8 Hz, 2H); 7.85 (d, J = 8.8 Hz, 2H); 4.69 (s, 2H; CH₂). ¹³C NMR (100.62 MHz, CDCl₃, 25°C, TMS): δ = 189.62; 136.84; 133; 128.89; 118.10; 117.31; 110.94; 42.3(CH₂). HRMS (ESI⁺) calcd for C₁₀H₇N₂OS [M+H] 203.0274, found: 203.0297.

p-Cyanophenacylselenocyanate (**2d**)

White solid. ¹H NMR (400.16 MHz, CDCl₃, 25°C, TMS): δ = 8.07 (d, J = 8.8 Hz, 2H); 7.85 (d, 2H, J = 8.4 Hz); 4.88 (s, 2H, CH₂). ¹³C NMR (100.62 MHz, CDCl₃, 25°C, TMS): δ = 192.1; 136.6; 133.0; 129.1; 118.1; 117.4; 101.0; 37.3(CH₂). ⁷⁷Se NMR (76.32 MHz, CDCl₃, 25°C, TMS): δ = 168.59. HRMS (ESI⁺) calcd for C₁₀H₅N₂OSe [M-H] 248.9562, found: 248.9560.

Cyclic voltammetry

The electrochemical reduction of the phenacylthiocyanates and phenacylselenocyanates (1 mM) were conducted in a three electrode glass cell, thermostated at 25 °C, under a dry nitrogen or argon atmosphere. The working electrode was a 2 mm diameter glassy carbon electrode (Tokai). It was carefully polished and ultrasonically rinsed with ethanol each time. The reference electrode was a SCE separated from the main solution by a fine porosity glass frit. The counter electrode was a platinum wire. A Metrohm Autolab instrument was used. Positive feedback correction was applied to minimize the ohmic drop between the working and reference electrode.

Theoretical Calculations

Optimizations were carried out using DFT at the B3LYP/6-31+G(d,p) level (and at the B3LYP/6-311+G(d,p) level for the sulphur and selenium atoms).³³ We checked that the conformations obtained were minima by running frequency calculations (no imaginary vibrational frequencies were found). Gas phase optimized energies for compounds **1a-c**, phenacyl radicals and [•]SCN and [•]SeCN were used to estimate homolytic bond dissociation energy values. LUMO calculation, geometries for one electron reduced compounds were calculated in DMF by using the PCM model. All energy values include zero point correction. The calculations were performed using the Gaussian09 package.³⁴ Z matrix and LUMOs for compounds **1a-e**, **2a-e**, radicals and radical anions are given in the SI.

Acknowledgements

Authors acknowledge *Ecos-Sud* (grant project A10E03), INFIQC-CONICET and Universidad Nacional de Córdoba (UNC). This work was partly supported by MINCYT-ECOS, CONICET, SECyT-UNC and FONCYT. Compound **5a** was kindly provided by F.R. Bisogno. LMB acknowledges CONICET for the receipt of a fellowship.

Notes and references

^a INFIQC-CONICET-UNC, Dpto. de Química Orgánica, Facultad de Ciencias Químicas, Universidad Nacional de Córdoba, Ciudad Universitaria, X5000HUA Córdoba, Argentina, *jea@fcq.unc.edu.ar, homepage <http://www.fcq.unc.edu.ar/infiqc>

^bUniversité Paris Diderot, Sorbonne Paris Cité,
Laboratoire d'Electrochimie Moléculaire, Unité Mixte de
Recherche Université - CNRS No 7591, Bâtiment Lavoisier, 15 rue Jean
de Baïf, 75205 Paris Cedex 13, France, *robert@univ-paris-diderot.fr

1. A. Houmam, *Chem. Rev.*, 2008, **108**, 2190-2237.
2. C. Costentin, M. Robert and J.-M. Savéant, *Chem. Phys.*, 2006, **324**, 40-56.
3. J.-M. Savéant, in *Advances in Physical Organic Chemistry*, ed. T. T. Tidwell, Academic Press, New York, 2000, vol. 35, pp. 117-192.
4. F. W. Maran, D. D. M.; Workentin M. S., in *Advances in Physical Organic Chemistry*, ed. T. T. Tidwell, Academic Press, New York, 2001, vol. 36, pp. 85-116.
5. A. Neumann, H. Scholz-Muramatsu and G. Diekert, *Arch. Microbiol.*, 1994, **162**, 295-301.
6. J.-M. Savéant, *J. Am. Chem. Soc.*, 1987, **109**, 6788-6795.
7. N. S. Hush, *Electrochim. Acta*, 1968, **13**, 1005-1023.
8. R. A. Marcus, *Electrochim. Acta*, 1968, **13**, 995-1004.
9. N. S. Hush, *J. Chem. Phys.*, 1958, **28**, 962-972.
10. R. A. Marcus, *J. Chem. Phys.*, 1956, **24**, 966-978.
11. R. A. Marcus, *J. Chem. Phys.*, 1965, **43**, 679-701.
12. K. B. Clark and D. D. M. Wayner, *J. Am. Chem. Soc.*, 1991, **113**, 9363-9365.
13. J.-M. Savéant, *J. Am. Chem. Soc.*, 1992, **114**, 10595-10602.
14. C. P. Andrieux, A. Le Gorand and J. M. Saveant, *J. Am. Chem. Soc.*, 1992, **114**, 6892-6904.
15. M. S. Workentin, F. Maran and D. D. M. Wayner, *J. Am. Chem. Soc.*, 1995, **117**, 2120-2121.
16. S. Antonello, M. Musumeci, D. D. M. Wayner and F. Maran, *J. Am. Chem. Soc.*, 1997, **119**, 9541-9549.
17. C. P. Andrieux, E. Differding, M. Robert and J. M. Saveant, *J. Am. Chem. Soc.*, 1993, **115**, 6592-6599.
18. A. Houmam and E. M. Hamed, *Chem. Comm.*, 2012, **48**, 11328-11330.
19. M. R. Claude P. Andrieux, Franklin D. Saeva, and Jean-Michel Savéant*, *J. Am. Chem. Soc.*, 1994, **116**, 7864-7871.
20. C. Ji, M. Ahmida, M. Chahma and A. Houmam, *J. Am. Chem. Soc.*, 2006, **128**, 15423-15431.
21. C. Ji, J. D. Goddard and A. Houmam, *J. Am. Chem. Soc.*, 2004, **126**, 8076-8077.
22. A. Houmam, E. M. Hamed, P. Hapiot, J. M. Motto and A. L. Schwan, *J. Am. Chem. Soc.*, 2003, **125**, 12676-12677.
23. A. Houmam, E. M. Hamed and I. W. Still, *J. Am. Chem. Soc.*, 2003, **125**, 7258-7265.
24. E. M. Hamed, H. Doai, C. K. McLaughlin and A. Houmam, *J. Am. Chem. Soc.*, 2006, **128**, 6595-6604.
25. R. H. B. Batanero, R. Mallmann, M.G. Quintanilla, F. Barba, *Electrochim. Acta*, 2002, **47**, 1761-1764.
26. M. a. D. Otero, B. Batanero and F. Barba, *Tetrahedron*, 2004, **60**, 4609-4612.
27. A. J. Mukherjee, S. S. Zade, H. B. Singh and R. B. Sunoj, *Chem. Rev.*, 2010, **110**, 4357-4416.
28. C. W. Nogueira, G. Zeni and J. B. T. Rocha, *Chem. Rev.*, 2004, **104**, 6255-6286.
29. G. Muges and H. B. Singh, *Chem. Soc. Rev.*, 2000, **29**, 347-357.
30. $\alpha = (RT/F)(1.85/E_{p/2} - E_p)$.
31. $\partial E_p / \partial \log(v) = -29.5/\alpha$ at 20°C.
32. F. R. Bisogno, A. Cuetos, I. Lavandera and V. Gotor, *Green Chem.*, 2009, **11**, 452-454.
33. A. D. Becke, *J. Chem. Phys.*, 1993, **98**, 1372-1377.
34. G. W. T. M. J. Frisch, H. B. Schlegel, G. E. Scuseria, M. A. Robb, J. R. Cheeseman, V. B. G. Scalmani, B. Mennucci, G. A. Petersson, H. Nakatsuji, M. Caricato, X. Li, H. P. Hratchian, A. F. Izmaylov, J. Bloino, G. Zheng, J. L. Sonnenberg, M. Hada, M. Ehara, K. Toyota, R. Fukuda, J. Hasegawa, M. Ishida, T. Nakajima, Y. Honda, O. Kitao, H. Nakai, T. Vreven, J. A. Montgomery, Jr., J. E. Peralta, F. Ogliaro, M. Bearpark, J. J. Heyd, E. Brothers, K. N. Kudin, V. N. Staroverov, T. Keith, R. Kobayashi, J. Normand, K. Raghavachari, A. Rendell, J. C. Burant, S. S. Iyengar, J. Tomasi, M. Cossi, N. Rega, J. M. Millam, M. Klene, J. E. Knox, J. B. Cross, V. Bakken, C. Adamo, J. Jaramillo, R. Gomperts, R. E. Stratmann, O. and A. J. A. Yazyev, R. Cammi, C. Pomelli, J. W. Ochterski, R. L. Martin, K. Morokuma, V. G. Zakrzewski, G. A. Voth, P. Salvador, J. J. Dannenberg, S. Dapprich, A. D. Daniels, O. Farkas, J. B. Foresman, J. V. Ortiz, J. Cioslowski, and D. J. Fox, *Gaussian 09, Revision D.01*, Gaussian, Inc., Wallingford CT, 2013.